FY14 Progress Report on Deep Borehole Material Degradation and Effects

M. Sutton, H. R. Greenberg

July 31, 2014

Disclaimer

This document was prepared as an account of work sponsored by an agency of the United States government. Neither the United States government nor Lawrence Livermore National Security, LLC, nor any of their employees makes any warranty, expressed or implied, or assumes any legal liability or responsibility for the accuracy, completeness, or usefulness of any information, apparatus, product, or process disclosed, or represents that its use would not infringe privately owned rights. Reference herein to any specific commercial product, process, or service by trade name, trademark, manufacturer, or otherwise does not necessarily constitute or imply its endorsement, recommendation, or favoring by the United States government or Lawrence Livermore National Security, LLC. The views and opinions of authors expressed herein do not necessarily state or reflect those of the United States government or Lawrence Livermore National Security, LLC, and shall not be used for advertising or product endorsement purposes.

This work performed under the auspices of the U.S. Department of Energy by Lawrence Livermore National Laboratory under Contract DE-AC52-07NA27344.

FY14 Progress Report on Deep Borehole Material Degradation and Effects

Used Fuel Disposition Campaign Milestone M4FT-14LL0817019

LLNL Input to a Multi-Laboratory Report on Deep Borehole Disposal Research:
Geological Data Evaluation, Alternative Waste Forms, and Borehole Seals

Mark Sutton and Harris Greenberg, LLNL

August 1st 2014

LLNL-TR-658009

Preface

This report satisfies the Lawrence Livermore National Laboratory Level 4 milestone (M4FT-14LL0817019) for the Deep Borehole Disposal Research area of the Used Fuel Disposition (UFD) Campaign, funded by the U.S. Department of Energy's Office of Nuclear Energy (DOE-NE). The work was performed under UFD work-package FT-14LL081701.

The following sections are to be inserted into a level-3 milestone report led by Sandia National Laboratories (SNL) – "Deep Borehole Disposal Research: Geological Data Evaluation, Alternative Waste Forms, and Borehole Seals" (M3FT-14SN0817021). LLNL is responsible for sections 3.4 (Degradation of Waste Canister Materials, Waste Forms and Drill Casing Materials) and 4.2 (Chemical and Physical Stability of Borehole Seals). Other sections written by other authors/institutions are excluded from this LLNL milestone report.

Table of Contents

List of Figures

List of Tables

Acronyms

A	surface area
DNFSB	Defense and Nuclear Facilities Safety Board
CNWRA	Center for Nuclear Waste Regulatory Analyses
CsCl	cesium chloride
DOE	U.S. Department of Energy
FCT	Fuel Cycle Technologies
HE	hydrogen embrittlement
L	length
LLNL	Lawrence Livermore National Laboratory
MCi	mega-Curies
MIC	microbially influenced corrosion
MPa	mega-Pascal
NE	Nuclear Energy
NWTRB	Nuclear Waste Technical Review Board
P	power
P_o	initial power
Q	decay heat
QA	Quality Assurance
SCC	stress corrosion cracking
SNL	Sandia National Laboratories
SrF_2	strontium fluoride
SS	stainless steel
t	time
$t_{1/2}$	half-life
T	temperature
$T_{surface}$	surface temperature
U	universal heat transfer coefficient
UFD	Used Fuel Disposition
W	Watts

3. Disposal System Design for Alternative Waste Forms

(Sections 3.0 to 3.3 are being written by other collaborators)

3.4 Degradation of Waste Canister Materials, Waste Forms and Drill Casing Materials

The components of the engineered barrier (from waste form to borehole liner) are shown as concentric circles in Figure 3.xx. (in section 3.x of the parent document authored by SNL). From the inside outwards, the disposal system design must consider degradation of waste form (including capsules and contents), waste package material (added before emplacement), drill casing (including conductor, surface, final and waste string casing) and cementing between the drill casing and host rock.

3.4.1 Degradation of Waste Forms

Before evaluating the degradation of the waste form ($CsCl$, SrF_2 and capsule materials), it is important to understand the chemical and thermal environment that capsules have been subject to, from filling and storage in a pool, to periodic inspection and future emplacement in a borehole.

3.4.1.1 High-Level Waste Material

A total of approximately 86 MCi of Cs-137 in the form of $CsCl$ was encapsulated by October 1983 and approximately 37 MCi of Sr-90 in the form of SrF_2 was encapsulated by January 1985 at the Hanford Waste Encapsulation and Storage Facility (Covey, 2012). Cs-137 undergoes beta decay with a half-life of 30.17 years forming barium-137m, which emits gamma photons (2.55 minute half-life) to form stable barium-137. Sr-90 undergoes beta decay with a half-life of 28.8 years to form yttrium-90, which then undergoes beta decay (64 hour half-life) and emission of an anti-neutrino to form stable zirconium-90. Decay-corrected to 2011, the total remaining activities of Cs and Sr are 38 MCi and 16 MCi, respectively (Covey, 2012).

Loading of $CsCl$ capsules was performed by pouring melted salt. The melting point of pure $CsCl$ is 645°C, and two different types of furnaces were used to melt the material – an induction furnace at a temperature of 730 to 750°C and later a tilt-pour furnace (DOE, 1990). On initial loading, the surface of the capsule was subjected to molten salt temperatures (<750°C), but surfaces quickly cooled as $CsCl$ solidified. The presence of impurities in $CsCl$ depresses its melting point. A review of total impurities for selected capsules (Tingey et al., 1983) shows that impurities may account for between 18-31%, including significant chloride salts of aluminum, barium, iron, potassium, sodium and silicon (DOE, 1990). Additionally, $CsCl$ undergoes a phase-change at 469°C which results in a 15% decrease in density on cooling in addition to the 9% change that occurs

on solidification below the melting point (DNFSB, 1996). Such changes in density led to a void volume in the poured salt. The actual temperatures experienced by the inner capsule during and after pouring CsCl could vary greatly depending upon the operator and the location of the inner capsule (DOE, 1990). After cooling and welding, inner capsules were cleaned with demineralized water and the surfaces were electopolished (DOE, 1990).

Processing temperatures (for example during vacuum tests) for CsCl capsules at the salt-metal interface were expected to not exceed 450°C (Heard et al., 2003) for periods of a few hours to a few days. Similarly, for SrF_2 capsules, processing temperatures at the salt-metal interface were not expected to exceed 540°C. SrF_2 melts at a much higher temperature (1477°C), so it is unlikely that any phase changes have occurred in the SrF_2 canisters. It is important to note that SrF_2 capsules also contain additional foreign materials beyond the simple salt, including metallic parts, ceramics and carbonaceous materials taken from floor and hot-cell deck operations (Bryan, Olander and Tingy, 2003), which complicate a full understanding of each SrF_2 capsule. Since SrF2 was not melted immediately prior to loading, the highest temperatures observed by the inner wall of the alloy C-276 inner capsules (and 316L outer capsules) result from the decay heat only.

3.4.1.2 Capsule Surface and Centerline Temperatures

To understand the temperatures experienced by the waste form (and the subsequent capsule degradation mechanisms), a first approximation of capsule centerline and surface temperature histories have been calculated for both air-cooled and pool-cooled environments.

The decay heat on 1/1/1995 and 1/1/2010 were provided in a presentation to the Nuclear Waste Technical Review Board (Randklev, 1994) for both Cs and Sr capsules, as well as the surface and centerline temperatures of the capsules. The same temperature data appears in Final Environmental Impact Statement (DOE, 1987).

The actual starting point in the transient temperature calculation (in time) is not critical, since the values are scaled according to the exponential decay of the waste heat in the Cs and Sr capsules. The surface and centerline temperatures given in DOE (1987) and Randklev (1994) were assumed to be design values. However, it was also assumed that the cooling air or water inlet temperatures and flow rates were adjusted to achieve these design temperatures given the decay heat as of January 1st, 1995. Assuming the cooling system input temperatures and flow rates were held constant, the heat transfer coefficients would also remain constant, and calculated results could be checked against the tabular values given for January 1st, 2010 and also calculated for different decay heat values at later times.

The thermal analysis for a preliminary design concept for a dry storage facility, which was prepared in 2003 (Heard et al., 2003), provided a basis for the decay heat of the capsules, scaling the capsule decay heat with the half-life of Cs capsules. Power decay

from the initial power level is based on the following equation, where P_0 is the initial power and Δt is the number of years to the calorimetric date:

$$P = P_0 \exp(-0.6931 \, \Delta t \, / \, t_{1/2})$$

The approach was to back-calculate equivalent universal heat transfer coefficients in air and water from the temperature results for 1995. An approximate steady state forced convection heat transfer situation was assumed with

$$Q = U*A*(T_{surface} - T_{ambient}), \text{ therefore}$$

$$U*A = Q/(T_{surface} - T_{ambient})$$

where Q = decay heat in W, and U*A is the universal heat transfer coefficient (in air or water) multiplied by capsule surface area in (final units are W/°C). Then, assuming U*A is held constant,

$$T_{surface} = T_{ambient} + U*A/Q$$

Radiation heat transfer was neglected, based on the assumption that a capsule would be located within a hot enclosure or hot array of capsules, so the radiation heat sink would have a similar temperature to source. A forced convection environment was assumed where cool ambient air at 22°C (site average ambient air temperature from Heard et al., 2003) or 50°C for water (DOE, 1990) is supplied to remove the heat, rather than relying on natural buoyant convection where the heat transfer coefficient would be a function of temperature difference. The Cs and Sr capsules have almost identical geometry, so the U*A function for both capsules should be approximately the same in each media, shown in Table 3-1.

Table 3-1 Calculated universal heat transfer coefficients for CsCl and SrF$_2$ capsule surface areas in air and water

Capsule	Decay Heat (W)	Surface T in Air (°C)	UA in Air (W/°C)	Surface T in Water (°C)	UA in Water (W/°C)
CsCl	165	200	0.9270	58	4.5833
SrF$_2$	273	430	0.6691	71	5.5714

To calculate the difference between surface and centerline temperature, constant capsule salt properties were assumed, ignoring heterogeneity and potentially temperature dependent salt thermal conductivity. The equation used for effective thermal conductivity is based on an analytical solution assuming uniform internal heat generation (Bird, Steward and Lightfoot, 2002),

$$K_{eff} (W/m/K) - Q/(4 \, \pi \, L \, (350 - T_{surface})$$

where Q is the total heat of the capsule in Watts, L is the length of the capsule in meters, and $T_{surface}$ is the surface temperature of the capsule in °C.

Following this approach, an effective capsule thermal conductivity was calculated using the surface and centerline temperatures for exposure in air, and then the effective thermal conductivity was used to calculate the centerline temperature in water. This approach predicted slightly lower than the design centerline temperatures in water, so a margin was added (around 6% for Cs and 12% for Sr) to adjust the predicted centerline temperatures in water to match the design values in 1995. The calculated effective thermal conductivity based on temperatures in air, and the predicted centerline temperatures in water in 1995 are shown in Table 3-2.

Table 3-2 Calculated effective CsCl and SrF$_2$ thermal conductivity at the centerline of capsules and calculated centerline temperature in water

Capsule	Centerline T in Air (°C)	Salt Keff (W/m/K)	Centerline T in Water (°C)	Calculated Centerline T in Water (°C)
CsCl	450	0.1048	327	308
SrF$_2$	860	0.1044	560	501

The first approximation of capsule temperature (centerline and surface) in air from 1995 to 2030 is shown in Figure 3-1, representing the maximum temperature that an average capsule would experience during inspection, vacuum check and inner capsule integrity (movement, "clunk") test (see section 3.4.1.5) and assumes equilibrium is reached between air and capsule.
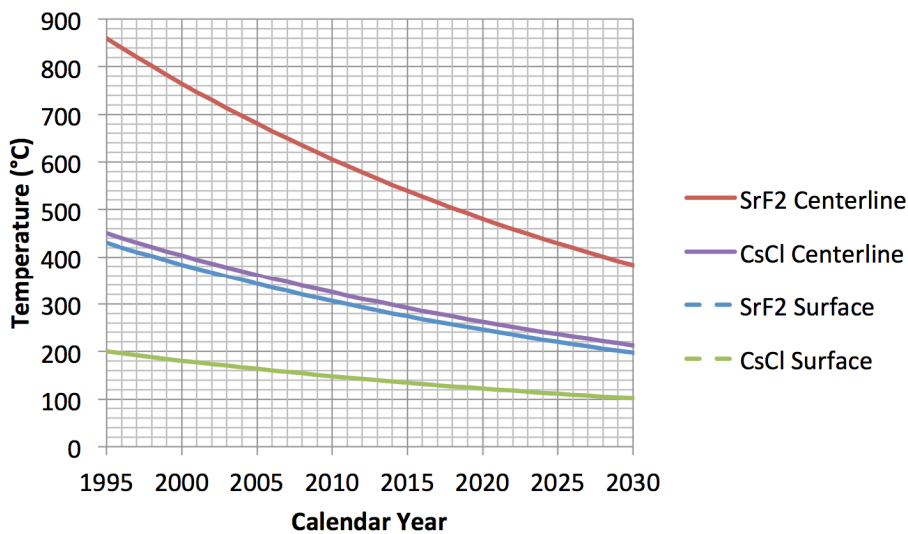
Figure 3-1. Predicted CsCl and SrF$_2$ capsule surface and centerline temperature transients in air

3.4.1.3 Storage Pool

Pool cell water is maintained below 50°C (DOE, 1990). A first approximation of the capsule temperatures (centerline and surface) in pool water is shown in Figure 3-2. The temperature of the capsule surface (when cooled by pool water) falls from 58 to 54 °C for CsCl capsules and from 71 to 59°C for SrF_2 capsules from 1995 to 2030.
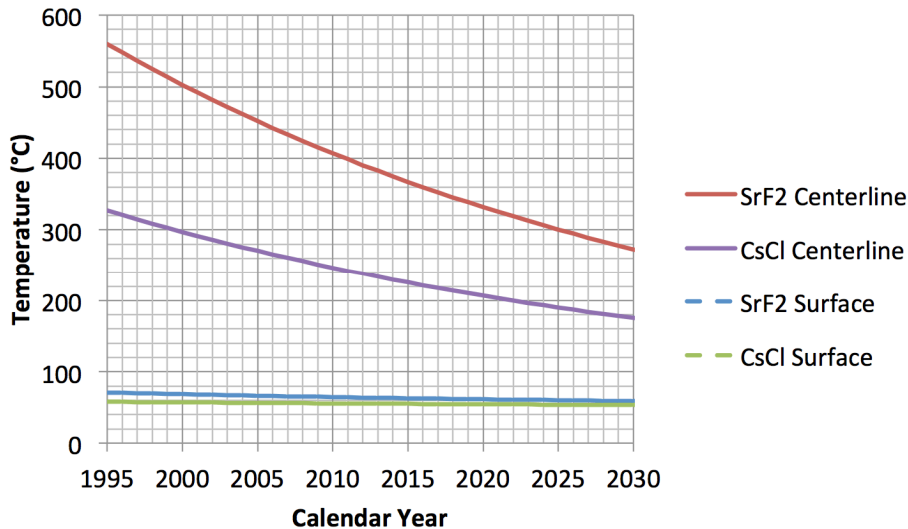
Figure 3-2. Predicted CsCl and SrF₂ capsule surface and centerline temperature transients in pool water

Figure 3-3 shows the first approximation of a temperature profile of the centerline and surface of capsules removed from the pool in 2019, stored in air and subsequently undergoing geologic disposal in 2020.
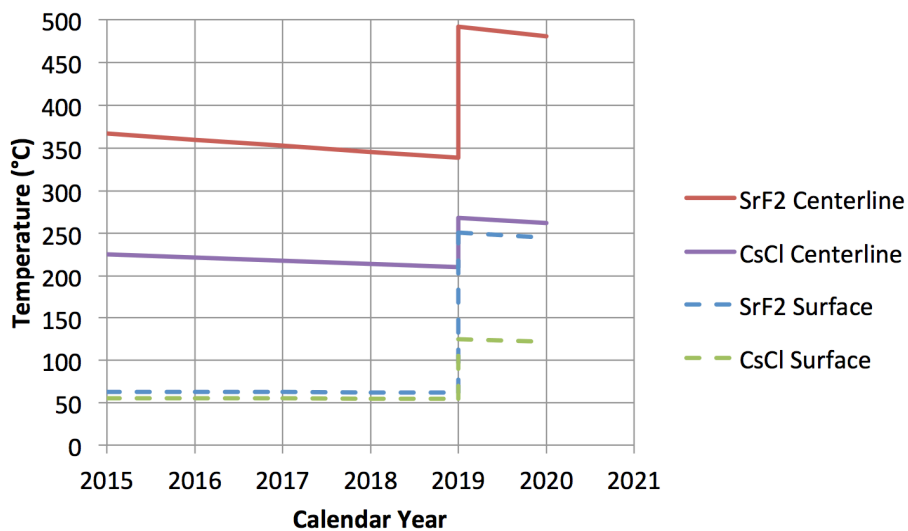
Figure 3-3. Predicted CsCl and SrF₂ capsule temperature transients for pool storage followed by removal to air storage in 2019 prior to disposal in 2020

The temperature histories for CsCl and SrF$_2$ capsules in both air-cooled and pool-cooled environments should be considered when determining degradation mechanisms of capsule materials (316L stainless steel and alloy C-276), particularly regarding thermal cycling and the effect that has on phase precipitation at grain boundaries and stress loading at weld locations. The potential for capsule corrosion may necessitate the use of overpacks and waste canisters prior to disposal.

3.4.1.5 Stored Capsule Material Degradation

Standard capsules containing CsCl are manufactured from an inner 316L stainless steel shrouded by an outer container of the same material. The Type W container is comprised of an additional single-layer 316L stainless steel overpack. SrF$_2$ capsules are comprised of Hastelloy C-276 inner layer and an outer layer comprised of either 316L stainless steel or Hastelloy C-276. The use of Hastelloy C-276 provides additional corrosion resistance over 316L against fluoride and fluorine, and has a lower average coefficient of thermal expansion (12.8[*] versus 16.2[†] microns per meter-Kelvin in the 0 to 315°C range).

The elemental composition of the two canister materials is given in Table 3-3 (SAE, 1986).

Table 3-3 Elemental composition of 316L stainless steel and alloy C-276

Composition wt%	C	Fe	Mn	Mo	Cr	Ni	Co	P	S	Si	W
316L	0.030	Bal (69)	2.00	2.00 to 3.00	16.00 to 18.00	10.00 to 14.00	-	0.045	0.030	1.00	-
C-276	0.02	4.0 to 7.0	1.0	15.0 to 17.0	14.5 to 16.5	Bal (57)	2.5	0.030	0.03	0.08	3.0 to 4.5

In austenitic stainless steels and nickel-based alloys such as SS-316L and C-276 where chromium is added to enhance corrosion resistance, chromium carbides (mainly $Cr_{23}C_6$) can precipitate at the grain boundary at temperatures between 425°C and 815°C. This leads to depletion of the passivating chromium metal in both the grain boundary and the grain body, a process known as sensitization, leading to areas with no passivity, which in-turn corrode preferentially. The capsule materials are then susceptible to inter-granular corrosion (IGC) as a result of elevated carbon content in the steel and sensitizing heat treatments (exposures). As discussed above, the temperature of CsCl-containing SS-316L capsules reached a maximum of 750 during melt-pouring. During vacuum testing, surface temperatures of SS-316L capsules containing CsCl were lower than the region of concern for IGC, with surface temperatures in air at or below 200°C from 1995 onwards and surface temperatures in water substantially lower. For C-276 capsules containing

---

[*] http://www.corrosionmaterials.com/documents/dataSheet/alloyC276DataSheet.pdf
[†] http://www.atlassteels.com.au/documents/Atlas316-316L.pdf

SrF$_2$, surface temperatures of 430°C were experienced on loading and during periodic inspection, leading to thermal cycling in the lower range of temperatures known to cause IGC.

Semi-annual inner capsule movement ("clunk") tests are performed on stored capsules, in which the integrity of the inner capsule is evaluated by shaking the capsule to move it while inside the outer capsule. If the inner capsule is swollen, it is assumed there will be no free movement within the outer capsule and no "clunk" will be heard. While most capsules are in good condition, 23 capsules required overpacks (NAS, 2003; DOE, 2002) potentially because of failing the "clunk" test. Capsule failure may occur because of poor welds and phase-changes as a function of temperature (NAS, 2003; DNFSB, 1996). A letter report by DNFSB (1995) further states that some capsules have experienced extreme thermal cycling. Such temperatures may include those that cause phase transition in both CsCl and 316L stainless steel.

The chemistry of the cooling pool is controlled using a deionizing system to remove removes impurities such as corrosion products, dissolved salts, chloride ions, and solid debris. This helps to maintain the pool cell water quality and minimize the potential for external corrosion of the capsules. For 316L, this results in a negligible rate of pitting corrosion. (Covey, 2012). However, since the capsules were welded, there is the potential for stress corrosion cracking to occur. DNFSB (1996) noted that some CsCl capsules stored in the pool may have experienced chloride-induced stress corrosion cracking near the outer capsule welds due to lack of water chemistry requirements and control. For the 23 capsules requiring overpacks, the 316L SS overpack has a corrosion allowance of 0.318 cm to protect against potential capsule leaks (Fluor, 2003). Overpack temperatures were predicted to be in the range of 200-225°C during normal operations. 316L SS (both capsule and overpack) is susceptible to SSC if exposed to water without proper purity control, particularly when capsules were leased to other facilities as irradiation sources (DNFSB, 1996). One capsule has suffered a through-wall crack, while another leak was attributed to a fabrication defect in the weld (DNFSB, 1996).

3.4.1.6 Waste Form Degradation in Boreholes

A deep borehole disposal design should include evaluation and selection of drill casing that is resistant to concentrated brines, capable of handling tensile stresses necessary for 4-5 km boreholes, and a disposal canister resistant to reducing potentials. The combination of these layered "barrier" materials in conjunction with grouting should prevent the degradation of the waste form in the borehole.

The peak temperatures at the canister wall are expected to be 145°C for a stack of 10 canisters each containing 2 capsules at a depth of 4 km using a bentonite backfill and disposal occurring in 2020. With a crushed granite backfill, the temperature is expected to peak at 185°C. Water circulation is assumed to be very limited.

Conditions down borehole for the Cs-137 and Sr-90 capsules are expected to be anoxic with elevated temperatures and brine concentrations. Corrosion of the 316L and C-276

capsules under these conditions will be most likely be at risk from chloride-induced stress corrosion cracking. If the disposal canister is breached, the CsCl and SrF_2 salts will be available to concentrated brines for subsequent dissolution. The room temperature solubility of CsCl is very high at 1910 g/l (Haynes, 2014), while that of SrF_2 is relatively low at 0.21 g/l. Simulated SrF_2 from WESF has a low solubility at room temperature (0.135 g/l), increasing slightly with temperature to 0.157g/l at 50°C (Fullam, 1976), but the dissolution rate of SrF_2 from WESF was dependent on surface area, impurity content, thermal history and temperature (amongst other factors). Given the saturated nature of the brine and its stagnant nature, it is feasible that these soluble salt waste forms may exhibit slower dissolution kinetics.

3.4.2 Selection of Disposal Canister Materials

At the elevated temperatures down-borehole, concentrated brines will dominate the water chemistry. In fact, leached sodium and chloride concentrations increase with temperature and depth (Anderson, 2004). For boreholes in granite, the pH is expected to be between 7 and 9), the redox potential between -200 and -300 mV (Rebak, 2006) and the major brine constituents may include 20 molal calcium, 100 molal chloride and 60 molal sodium (Anderson, 2004).

The chemical environment within the borehole, namely reducing potential, fairly neutral pH and high brine concentrations may allow the use of copper disposal canisters encasing the steel capsules. Canisters may be constructed of copper, or steel with copper deposited on the surface by either cold-spray or electroplating. Copper is favored in some European repository designs and the use of copper coating over steel is under investigation in Canada. It should also be noted that several grades of copper-based alloys are single-phased up to 300°C (Bullen and Gdowski, 1988), which suggests that phase stability should not be a problem in deep boreholes. A report by CNWRA (Winterle, Pauline and Ofoegbu, 2011) notes that the demand for copper as an economic resource might cause future problems and Vicente (2007) proposed lead as an alternative canister material.

A comparison of steels, alloys and pure metals is required that includes consideration of material and construction cost, corrosion resistance, mechanical properties and future economic value is required.

3.4.3 Selection and Degradation of Drill Casing Materials

3.4.3.1 Drill Casing / Borehole Liner

Standard drill casing is available in a variety of steels, ranging from carbon steels (e.g. J55, K55, N80, H40 and P110) to L80, C95 and T95 high strength low alloy (HSLA) steels. These steels are generally used for severe sour well applications where exposure of high partial-pressure of hydrogen sulfide (H_2S) environments can lead to pitting

corrosion and stress corrosion cracking (SCC) in standard drill casing materials. The elemental composition, minimum tensile strength and minimum yield strength of these steels are given in Table 3-4 (source: http://www.contalloy.com/gradefinder/)

Table 3-4 Elemental composition and minimum tensile and yield strengths for commonly used drill pipe including carbon and high strength low alloy steels

Max composition	C	Mn	Mo	Cr	Ni	Cu	P	S	Si	Tensile Strength, MPa min.	Yield Strength, MPa min.
Carbon Steels incl. J55, K55, N80, H40, Alloy P110	-	-	-	-	-	-	0.030	0.030	-	J55: 517 K55: 655 N80: 689 H40: 414 P110: 862	J55: 379 K55: 379 N80: 552 H40: 276 P110:758
L80 Alloy (HS res)	0.43	1.90	-	-	0.25	0.35	0.03	0.03	0.45	655	552
T95 and C90 Alloy (HS SSC res)	0.35	1.20	0.85	1.50	0.99		0.02	0.01		T95: 724 C90: 689	T95: 655 C90: 621

Based on tensile and compressive stress calculations for a number of borehole steel drill casing materials examined in Hoag (2006), C95 or T95 alloy is required to support a 2 km emplacement zone in a 4 km borehole using a reference design PWR waste string of ~921 metric tons (resulting in a tensile stress of 720 MPa). For Cs/Sr capsules, the waste string mass (capsules, contents and waste packages) requires calculation to determine whether L80 alloy is suitable in addition to C90 and T95 alloys. In addition, Hoag (2006) references (Berger and Anderson, 1992) suggesting that H40, J55 or K55 conductor casing and surface casing could be used with H40 final casing and J55 or P110 casing for the waste string.

In addition to considering tensile and compressive stresses, other important factors to consider when selecting drill casing for deep borehole liner include phase stability and aging, stress corrosion cracking, hydrogen embrittlement and microbially influenced corrosion. We also consider delamination as a degradation mechanism.

While phase stability is not a significant issue for the drill casing materials at temperatures predicted for boreholes (185°C), long-term aging of the drill casing at elevated temperatures (50-250°C) is potential concern, especially when considering the long time-periods involved in borehole disposal. Over the course of 300-1000 years, precipitation of carbides and inter-metallic compounds can occur, which may adversely reduce the passivity. It is important to note here that this is also a major concern for SS316L and C276 alloys.

Microbially influenced corrosion (MIC), particularly by the action of sulfate-reducing bacteria that can exist in anoxic environments is known to affect stainless steels,

austenitic alloys, carbon steels and high-strength low-alloy steels. However, the effects of MIC tend to decrease above 65°C (Kumar and Anand, 1998) and the bacteria is typically neutralized at approximately 95°C (Kallmeyer and Boetius, 2004). Since borehole emplacement temperatures are likely to remain above 100°C due to geothermal temperatures alone, the likelihood of MIC affecting drill casing in the emplacement zone (or disposal canisters and capsules for that matter) is low.

Hydrogen embrittlement (HE) is caused by atomic hydrogen from the environment (formed by electrons generated during a corrosion process reacting with hydrogen ions from water) entering the steel. HE is one of the major corrosion mechanisms for high-strength low alloy steels. At relatively low temperatures, the atomic hydrogen in the steel combines with other atoms of hydrogen, forming hydrogen gas bubbles. As more gas bubbles form, the pressure inside the metal structure increases causing reduced ductility and tensile strength, finally resulting in the formation of cracks. At higher temperatures, the hydrogen atom combines with carbon in the steel to form methane. The HE process in steel is most susceptible at high ambient temperatures and tends to decrease at higher temperatures such as those experienced in deep boreholes. The presence of chloride brines can greatly increase the general corrosion of steels, which in turn increases the availability of hydrogen for HE. The presence of sulfide in the borehole hinders the atomic hydrogen recombination reaction, causing more hydrogen to enter the steel and increasing HE. Generally, the higher the yield stress of the steel, the more susceptible it is to HE, making alloys such as T95 and C90 more prone to HE than carbon steels such as H40, J55 and K55.

Stress corrosion cracking (SCC) requires three factors, namely (i) stress (either through weld or tensile/compressive from borehole component mass), (ii) a flaw (crack, initiation site) and (iii) a material-specific corrosive environment. A flaw can be a pre-existing condition due to poor manufacturing or can be initiated in locations where a high-stress concentration exists such as grooves or corrosion pits (Farmer et al., 1999). The highly concentrated brine solutions present in a deep borehole are certainly capable of causing a corrosive environment for some steels (including carbon steels), but high-strength low-alloys steels such as T95, C90 and L80 are not particularly susceptible to chloride-induced SCC. A greater concern for these alloys, particularly in the anoxic environment of the emplacement zone in deep boreholes is hydrogen embrittlement or microbially influenced corrosion (MIC) together with stress causing *environmentally assisted cracking*.

The possibility of the formation of lamellar corrosion products through the exfoliation/delamination of the drill casing or waste package has been proposed. This process occurs when the corrosion products (metal oxides) become several time greater in volume that the original metal, leading to the formation of internal tensile stresses which effectively tear apart the material into sheets (lamella). The layers between each sheet may serve as a vertical pathway for radionuclides within the borehole perimeter. Delamination can also occur due to differences in thermal expansion of oxides and metal. This type of corrosion is considered to be unlikely to occur on the surface both 316L stainless steel and C-276 alloy. Low alloy steels such as those proposed for drill casing

(e.g. L80 and T95) are susceptible to delamination. Furthermore, steels fabricated by extrusion or rolling contains flat or elongated grains, which are prone to inter-granular corrosion, and thus leading to lamellar corrosion products. However, given the anoxic potentials considered for deep boreholes, it is unlikely that delamination will occur in any of the metals down borehole because of the absence of oxygen (and therefore the absence of oxide corrosion products).

4 Borehole Seals Research and Planning

(Sections 4 and 4.1 will be written by SNL)

4.2 Thermal and Chemical Stability of Borehole Seals

The two key phenomena that affect the mechanical stability of borehole seals (and hence their performance in preventing both flow of pore water to the waste container and release of radionuclides to the environment) are the temperature and chemical environment in contact with the seals. These phenomena are evaluated with respect to various alternative designs for cement, bentonite and asphalt seals. Bentonite seals have many advantageous properties, including low permeability, high sorption capacity, self-sealing characteristics and durability (Brady et al., 2009). Above the emplacement zone, the use of bentonite, asphalt and concrete is considered (Brady et al., 2009), as is the method proposed by Gibb et al. (2008a) of using crushed host-rock. Concrete has low permeability and is widely used in hydraulic applications including sealing the wellbore to host-rock and surface. The extensive review of Pabalan et al. (2009) discusses important characteristics of cement degradation relevant to engineered barriers used in radioactive waste disposal. Asphalt is used to prevent water migration down the borehole and its properties include strength, adhesion, water-resistant, durable and placicity (Brady et al., 2009). Additional sealing concepts including emplacement zone metallic backfill (e.g. lead-based alloys) for lower temperature designs and waste canisters with a high specific gravity (8-11), (Gibb 2008b) and a slurry of granite resulting in partial rock melting and recrystallization in higher temperature designs (Gibb 2008b) are not considered in this review.

The temperature gradient for borehole disposal may range from ambient temperature at the surface to 75°C in the upper portion and 150-200°C in the emplacement zone. The effects of such temperatures on asphalt and cement seals is expected to be minimal. However, the drying of bentonite at these temperatures will lead to shrinking and cracking in unsaturated zones. In deeper regions of the borehole, above temperatures usually associated with clay dehydration under less harsh conditions, hydrostatic pressure should prevent hydrated bentonite from drying and cracking.

The volume of bentonite is reduced over time during conditions likely to occur in a deep borehole. The high ionic strength associated with deep brines and the presence of

divalent cations including Ca^{2+}, Mg^{2+} and Fe^{2+} from the host rock (and additionally Fe^{2+} and Ni^{2+} from the anoxic corrosion of drill casing) cause displacement of cations in the sheet silicates of clay. The resulting shrinkage of bentonite can lead to voids in the seal and allow both potentially harmful brines to reach the waste canister and allow the migration of radionuclides from the waste form. Additionally, the impact of cement leachate (resulting in a high pH conditioned solution of mono- and di-valent cations including Na^+, K^+ and Ca^{2+}) may play in important role in the long-term chemical stability of bentonite. Recent work by Caporuscio et al. (2014) in which bentonite was placed in contact with Opalinus clay host rock, groundwater and metal coupons (including 316 stainless steel) at elevated temperatures (120 to 300°C) and pressures ($\leq$ 16 MPa) showed a decrease in the pH, K^+ and Ca^{2+} concentrations in porewater and an increase in aqueous silica, sodium and sulfate. Caporuscio et al. (2014) also noted that reaction kinetics were accelerated under water saturation and that illitization did not occur within the bentonite fraction. Additional work proposed by Caporuscio (2014), particularly including the use of both mafic (amphibolites) and silicic (granitic gneiss) end-members, would provide key data that could integrate geochemical modeling efforts from other areas of the UFD campaign.

Cement can undergo both chemical and physical degradation. Chemical degradation may include reaction with gaseous or dissolved carbon dioxide (carbonation) leading to precipitation of $CaCO_3$ and consequently a reduction in the ratio of Ca:Si in the calcium-silicate-hydrate (CSH) matrix. Pabalan (2009) points out that while carbonation does not have a significant macro-structural effect, the indirect effect is a reduction in pH buffering from cement, which can adversely influence steel corrosion. Sulfate ions can also lower the Ca:Si ratio by precipitation of calcium sulfate minerals (and magnesium hydroxide in the presence of a source of Mg^{2+} ions), which are generally larger in volume than the CSH matrix, resulting in expansion, disintegration and loss of strength, termed "sulfate attack" (Pabalan, 2009). Carbonation and sulfate attack represent potentially the most relevant chemical degradation mechanisms in a deep borehole environment. The processes are further described in Poole et al. (1993), Tumidajski and Chan (1996) and Wakeley et al. (1993). Such processes are not well understood at temperatures, pressures and brine concentrations at emplacement depth. Recent work by Carroll et al. (2011) and Walsh et al. (2014) have combined experimental studies and modeling to understand such processes relevant to geologic carbon sequestration conditions, and the work highlights the need for close integration between deep borehole disposal and other areas of deep geologic exploration, including oil, gas, geothermal and carbon sequestration.

Other chemical degradation mechanisms of cement include leaching of soluble components, such as $Ca(OH)_2$ and minerals of silicate and aluminate, enhanced by neutral to low pH. Corrosion of steel products in the vicinity of cement may also lead the formation of iron oxides of higher volume that in turn cause cracking and loss of strength similar to carbonation.

The basis for cement longevity at the Waste Isolation Pilot Plant (WIPP) was determined for borehole plugs in experiments conducted by Thompson et al. (1996) who found that plug failure occurred when the calcium-silicate-hydrate (CSH) matrix undergoes

measurable alteration. Thompson also concludes that in a 3-plug borehole design, deeper casing corrosion will be less severe than upper sections and that deeper plugs (e.g. 4 km) will not fail for approximately 5,000 years.

Asphalt is primarily a complex mixture of high molecular-weight hydrocarbons, sometimes containing compounds of iron, silicon and aluminum. Aggregates may be used in asphalt to add strength and may include granite amongst other minerals. Asphalt is widely used (and greatly researched) in terms of road construction, and asphalt has been used for many centuries. Stieter and Snoke (1936) observed the formation of water-soluble asphalt degradation products in the presence in oxic environments exposed to light. However, the relatively benign upper environment in the top 250 to 500 m of the borehole precludes UV light from breaking down the organic constituents in asphalt, while any contacting water will be dilute in nature rather than the concentrated brines observed in the emplacement zone, and conditions will be mildly anoxic. Such conditions will prevent the degradation of asphalt for a long period of time. Microbial activity is known to degrade asphalt, with chemical environment, pH and redox conditions affecting the growth and effects (Phillips and Traxler, 1963). Additionally, the organic content of the asphalt may provide nutrients for microbes to grow, and the sulfur present in asphalt may provide a source for sulfate-reducing bacteria known to influence corrosion (MIC). Degradation studies of asphalt under borehole conditions (particularly in regard to MIC) is recommended.

~

Sections 5 and 6 are being written by other collaborators

7.0 References

Anderson, V.K. 2004, An Evaluation of the Feasibility of Disposal of Nuclear Waste in Very Deep Boreholes, Thesis, MIT Department of Nuclear Science and Engineering, Sept. 2004.

Berger, B.D. and K.E. Anderson, 1992, Modern Petroleum - A basic primer of the industry, PennWell Publishing Company, Tulsa, Oklahoma.

Bird, R.B, W.E. Steward and E.N. Lightfoot, Transport Phenomena, 2nd Edition, 2002

Brady, P.V., B.W. Arnold, G.A. Freeze, P.N. Swift, S.J. Bauer, J.L. Kanney, R.P. Rechard, and J.S. Stein. Deep Borehole Disposal of High-Level Radioactive Waste, SAND2009–4401. Albuquerque, New Mexico: Sandia National Laboratories. 2009.

Bryan, G.H., D.R. Olander and G.L. Tingey 2003, Corrosion Report for Capsule Dry Storage Project, WMP-16937, September 2003 Fluor Hanford Inc., Richland, Washington.

Bullen, D.B. and G.E. Gdowski 1988, Survey of Degradation Models of Candidate Materials for High-Level Radioactive-Waste Disposal Canisters: Phase Stability, UCID-21362 Vol.1, August 1988, Lawrence Livermore National Laboratory, Livermore, California.

Caporusico, F.A., M.C Cheshire, M.S. Rearick and C. Jove-Colon 2014, LANL Argillite EBS Experimental Program 2014, FCRD-UFD-2014-000491 (LA-UR-14-25179), July 2014, Los Alamos National Laboratory (LANL), Los Alamos, New Mexico.

Carroll. S.A., W.W. McNab and S.C. Torres 2011, Experimental study of cement - sandstone/shale – brine – CO_2 interactions, Geochemical Transactions 12.

Covey, L.I., 2012, Waste Encapsulation and Storage Facility Documented Safety Analysis, DSA HNF-8758-07, Revision 7, Chapter 2, CH2MHill Plateau Remediation Company, Richland, Washington

Defense and Nuclear Facilities Safety Board (DNFSB), Hanford – B Plant/Waste Encapsulation and Storage Facility Review, Defense Nuclear Facilities Safety Board, Washington DC, 1995

Defense and Nuclear Facilities Safety Board (DNFSB), Trip Report—Safety of Cesium and Strontium Capsules at Hanford. Washington, D.C.: Defense Nuclear Facilities Safety Board. June 7th, 1996

Farmer, J., D. McCright, J-S. Huang, A. Roy, K. Wilfinger, R. Hopper, F. Wang, P. Bedrossian, J. Estill and J. Horn February 1999, Development of Integrated Mechanistically-Based Degradation Model Models for Performance Assessment of High-Level Waste Containers, UCRL-ID-130811 Rev 1, Lawrence Livermore National Laboratory, Livermore California.

Fluor 2003, Performance Specification for Capsule Dry Storage Project Design and Fabrication, HNF-16138 Rev 1, Fluor Hanford Inc., Richland, Washington.

Fullam, H.T. The Solubility and Dissolution Behavior of $^{90}SrF_2$ in Aqueous Media, Battelle Pacific Northwest Laboratories report BNWL-2101, November 1976, Richland Washington

Gibb, F.G.F., K.J. Taylor, and B.E. Burakov. "The 'Granite Encapsulation' Route to the Safe Disposal of Pu and Other Actinides." Journal of Nuclear Materials. Vol. 374, No. 3. pp. 364–369. 2008a.

Gibb, F.G.F., N.A. McTaggart, K.P. Travis, D. Burley and, K.W. Hesketh. "High-Density Support Matrices: Key to the Deep Borehole Disposal of Spent Nuclear Fuel." Journal of Nuclear Materials, Vol. 374. pp. 370–377. 2008b.

Haynes, W.M. (ed) Handbook of Chemistry and Physics 95th Ed 2014-2015, CRC, available at http://www.hbcpnetbase.com/

Hoag, C.I. "Canister Design of Deep Borehole Disposal of Nuclear Waste," Thesis, MIT Department of Nuclear Science and Engineering, September 2004.

Heard, F.J., K.R. Robertson, J.E. Scott, M.G. Plys, S.J. Lee, and B. Malinovic 2003. *Thermal Analysis of a Dry Storage Concept for Capsule Dry Storage Project*, WMP-16940, Flour Hanford, Richland, Washington

Kallmeyer, J. and A. Boetius□2004, Effects of temperature and pressure on sulfate reduction and anaerobic oxidation of methane in hydrothermal sediments of Guaymas Basin, *Applied Environmental Microbiology* 70(2):1231.

Kumar, C. and S. Anand, 1998, Significance of microbial biofilms in food industry: a review. International Journal of Food Microbiology, 42(9): 27.

National Academies of Science (NAS) National Research Council, 2003, *Improving the Scientific Basis for Managing DOE's Excess Nuclear Materials and Spent Nuclear Fuel*, The National Academies Press, Washington, DC.

Pabalan, R.T., F.P. Glasser, D.A. Pickett, G.R. Walter, S. Biswas, M.R. Juckett, L.M. Sabido and J.L. Myers, 2009, Review of Literature and Assessment of Factors Relevant to Performance of Grouted Systems for Radioactive Waste Disposal, CNWRA 2009-001, April 2009, Center for Nuclear Waste Regulatory Analyses (CNWRA), San Antonio, Texas.

Phillips, U.A and R.W. Traxler, 1963, Microbial degradation of asphalt, Applied Microbiology, 11(3):235.

Poole, T. S., L.D. Wakeley and C.L. Young, 1993, Individual and Combined Effects of Chloride, Sulfate, and Magnesium Ions on Hydrated Portland-Cement Paste: Sandia National Laboratories, Albuquerque, New Mexico.

Randklev, E., 1994, Disposal of Hanford site cesium and strontium capsules, presentation to the Nuclear Waste Technical Review Board (NWTRB), June 15th, 1994, TWRS Vitrification Development Tank Waste Remediation System, Westinghouse Hanford Company, Richland, Washington.

Rebak, R.B. 2006, Selection of corrosion resistant materials for nuclear waste repositories, *Materials Science and Technology,* Cincinatti, October 15-19, 2006. Also available as LLNL report UCRL-PROC-221893, June 8th 2006, Livermore California.

Society of Automotive Engineers (SAE) 1986, Metal and Alloys in the Unified Numbering System, 4th Edition, Society of Automotive Engineers, Inc., Warrendale, PA

Strieter, O.G. and H.R. Snoke 1936, A modified accelerated weathering test for asphalts and other materials, RP886, J. Research NBS, 17, 481 RP886

Thompson, T.W., W.E. Coons, J.L. Krumhansl, and F.D. Hansen (1996), Inadvertent Intrusion Borehole Permeability. ERMS 241131. Sandia National Laboratories, Albuquerque, New Mexico.

Tingey, G.L., E.J. Wheelwright and J.M. Lytle, A Review of Safety Issues that Pertain to the use of WESF Cesium Chloride Capsules in an Irradiator, PNL-5170 July 1983, Pacific Northwest National Laboratories, Richland Washington.

Tumidajski, P. J. and G.W. Chan, 1996, Durability of high performance concrete in magnesium brine: Cement and Concrete Research, v. 26, no. 4, p. 557-565

U.S. Department of Energy (DOE) 1987 *Final Environmental Impact Statement - Disposal of Hanford Defense High-level, Transuranic and Tank Wastes*, 1987 EIS-0113, Volume 2 of 5, Section 3, U.S. Department of Energy, Washington, DC.

U.S. Department of Energy (DOE), 1990, Interim repot of the DOE Type B investigation group; Cesium-137: A systems evaluation, encapsulation to release at Radiation Sterilizers, Inc., DOE/ORO--914, July 1990, U.S. Department of Energy, Washington, DC.

U.S. Department of Energy (DOE) 2002, Waste Encapsulation Storage Facility (WESF) fact sheet, REG-0275, U.S. Department of Energy, Richland Operations Office (ROO), Richland, Washington.

Vicente, R. 2007 Qualitative performance assessment of a borehole disposal system, Proceedings of the Waste Management 2007 Conference, Tucson, Arizona, February 25– March 1, 2007.

Wakeley, L. D., T.S. Poole, J.J. Ernzen and B.D. Neeley, 1993, Salt Saturated Mass Concrete Under Chemical Attack, *in* Zia, P., ed., High Performance Concrete in Severe Environments, Volume SP-140: Detroit, MI, American Concrete Institute.

Walsh, S.D.C. H.E. Mason, W.L. Du Frane and S.A. Carroll, 2014a, Experimental calibration of a numerical model describing the alteration of cement/caprock interfaces by carbonated brine. International J. Greenhouse Gas Control, 22, 176−188.

Walsh, S.D.C. H.E. Mason, W.L. Du Frane and S.A. Carroll, 2014b, Mechanical and hydraulic coupling in cement-caprock interfaces exposed to carbonated brine. International J. Greenhouse Gas Control, 25, 109−120.

Winterle, J., R. Pauline and G. Ofoegbu, 2011, Regulatory Perspectives on Deep Borehole Disposal Concepts, Center for Nuclear Waste Regulatory Analyses (CNWRA), San Antonio, Texas, May 2011.